Mechanical properties, glass transition temperature, and bond enthalpy trends of high metalloid Fe-based bulk metallic glasses

X. J. Gu,[1] S. Joseph Poon,[1,a)] Gary J. Shiflet,[2] and Michael Widom[3]
[1]*Department of Physics, University of Virginia, Charlottesville, Virginia 22904-4714, USA*
[2]*Department of Materials Science and Engineering, University of Virginia, Charlottesville, Virginia 22904-4745, USA*
[3]*Department of Physics, Carnegie Mellon University, Pittsburgh, Philadelphia, Pennsylvania 15213, USA*

Mechanical properties and glass transition temperatures (T_g) of Fe–Cr–Mo–P–C–B bulk metallic glasses containing up to 27 at. % metalloids have been studied. The shear modulus (G) is found to decrease with increasing metalloid content and a maximum plastic strain of ~3% is obtained, despite the increase in the number of strong metal-metalloid bonds. Also, T_g increases with the decrease in G, in contrast to usual behavior. By employing first-principles calculations, the results are discussed in light of atomic bonding and connectivity in the amorphous network. The findings are relevant to understanding ductility and glass transition of metallic glasses. © *2008 American Institute of Physics*. [DOI: 10.1063/1.2917577]

The deformation and rheological properties of metallic glasses are well described by the shear models.[1,2] It has been known for some time that shear modulus is an important parameter for determining the deformation behavior of metallic glasses. Chen *et al.* first reported that ductile metallic glasses tended to have a large Poisson's ratio (ν), or a lower shear modulus (G) to bulk modulus (K) ratio.[3] Recently, a critical ν for the onset of ductility in metallic glasses has been identified,[4] and the relationship between ductility and ν for several bulk metallic glasses (BMGs) has been studied.[5–8] In the deeply undercooled liquid, the activation barrier for viscous flow is proportional to G.[1,2] Correlations between glass transition temperature (T_g) and elastic moduli have also been observed.[1,9–12] While studies to date have focused on the metallic systems, the effects of strong chemical bonds inherent to many of the BMGs have not been addressed. Fe-based BMGs, which consist of both metallic and covalent bonds, can provide a unique system for studying chemical bond effects on properties. By varying the metalloid content and bond strength, such study can lead to a deeper understanding of the role of chemical bonds on physical properties of BMGs, which in turn can help to bridge the gap between metallic and covalent glasses.

In this paper, the effects of high metalloid content on mechanical properties and T_g of Fe–Cr–Mo–P–C–B BMGs are reported. The interdependences between G, T_g, and metalloid content follow unexpected trends. Combining first-principles electronic structure calculations and measurements, the results are interpreted in terms of alloying effects on chemical bond strengths in the amorphous network. Similar effects may also play a role in other BMG alloys. Alloy ingots were produced by arc melting a mixture of high purity Fe, Cr, Mo, C, B, and prealloyed Fe_3P under a Ti-gettered argon atmosphere. BMG samples, in the form of 1.5–2 mm diameter rods, were prepared by copper-mold suction casting under an argon atmosphere. The amorphicity of these cast samples was confirmed by x-ray diffraction (Cu $K\alpha$). Ther-

mal behavior of the samples were investigated in a differential scanning calorimeter (DSC) at a constant heating rate of 0.33 K/s. Room-temperature compression tests were performed on 1.5 mm diameter by 3 mm long rods using an Instron testing machine at a strain rate of 10^{-4} s^{-1}. Elastic moduli were measured by resonant ultrasound spectroscopy.[7,13] *Ab initio* electronic structure calculations were performed to provide clues as to the origin of the observed unusual T_g-G-metalloid content relations. Chemical bond effects in several crystalline phases namely Fe_3P (Pearson type tI32 structure), Fe_3B, and Fe_3C (both oP16), and also elemental Fe (cI2) were investigated using the methods previously reported.[13] The structures were relaxed using the VASP program.[14] The band structures were calculated using an linear muffin-tin orbital method[15] to provide the local orbital projections needed for the crystal orbital Hamiltonian population (COHP) calculation.[16] The COHP, integrated up to the Fermi level (ICOHP), is a measure of the covalent (shared electron) contribution to interatomic bonding.

The amorphicity of the alloys has been confirmed by x-ray diffraction and thermal analysis. With the exception of $Fe_{60}Cr_3Mo_{10}C_{10}B_3P_{14}$, which can only form 1.5 mm diameter glassy rods, all other alloys can be cast into glassy rods with diameter of 2 mm. DSC traces of several $Fe_{74-x}Cr_3Mo_{10}C_{10}B_3P_x$ glassy alloys are shown in Fig. 1. Clear glass transition and crystallization events are observed in the DSC scans. T_g and T_x, the crystallization onset temperature, for all the alloys studied are summarized in Table I. The overall trends indicate that both T_g and T_x principally increase with increasing total metalloid content. The mechanical properties of the present alloys are also listed in Table I. G is plotted as a function of total metalloid content in Fig. 2, which shows that G continues to decrease as the metalloid content increases from 19 to 27 at. %. In assessing the metalloid effect on the observed shear modulus trend, it is noted that the changes in G are rather small when C is substituted by B at the total metalloid content of 24 at.% (Table I and Fig. 2). The variation in G is therefore mainly due to changes in the total metalloid content. T_g is plotted as a function of G in Fig. 3. In contrast to the results reported for other alloys that showed increases in T_g with both in-

---

a)Author to whom correspondence should be addressed. Electronic mail: sjp9x@virginia.edu.
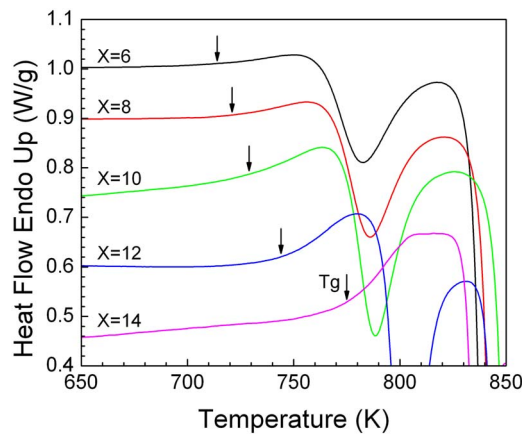
FIG. 1. (Color online) DSC curves showing glass transition and crystallization onsets of $Fe_{74-x}Cr_3Mo_{10}C_{10}B_3P_x$ (x=6, 8, 10, 12, and 14) glassy alloys.

FIG. 2. (Color online) Shear modulus (G) vs total metalloid content for Fe-BMGs listed in Table I.

creasing G and Young's modulus (E),[9–12] T_g decreases with increasing G and E (Table I) for the present alloys having a high metalloid content. Overall, G decreases while T_g increases with the increase in metalloid content (inset of Fig. 3), and inferably also with an increase in metal-metalloid bond number. The true compressive stress-strain (s-s) curves of several alloys are shown in Fig. 4. The yield stress σ_y is defined by the deviation from the linear part of the s-s curve, and the plastic strain ε_{pl} is estimated from the nonlinear part of the s-s curve. The current Fe-BMGs exhibit high yield and fracture strengths reaching 3.1 and 3.5 GPa, respectively, and high plastic strains up to 3.2%. The appreciable plasticities observed are consistent with the fact that these alloys have Poisson's ratios higher than the critical value of 0.31–0.32.[4,6,7]

The different degrees of covalency observed in iron-metalloid phases[13] suggest that there exists considerable heterogeneity of bond type and bond strength in Fe-(PCB) phases, which is confirmed in a preliminary study of Fe-(PCB) type BMGs. *Ab initio* study reveals effects of high metalloid content on Fe–Fe and Fe-metalloid bond strengths. As an example, Fig. 5 illustrates the ICOHP versus interatomic distance for Fe–Fe and Fe–P bonds in $Fe_3P \cdot tI32$ as compared with $Fe \cdot cI2$. At the metal-metal and metal-metalloid interatomic distances of interest, the Fe–P bonding enthalpy is clearly higher than the Fe–Fe bonding enthalpy. Equally noteworthy, however, is the finding that the Fe–Fe bond is actually weakened in proximity to P. Similar ICOHP versus interatomic distance trends for Fe–Fe and Fe-
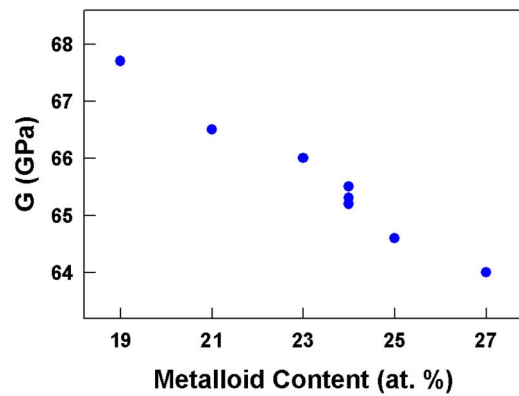
metalloid bonds occur in Fe–B and Fe–C, and the weakening of the Fe–Fe bonds becomes more pronounced as the total metalloid content increases. Further, the ICOHP trend of Fe–Mo is similar to that for Fe–Fe in the presence of metalloids.

The metal-metalloid bonds are strongly covalent and thus should resist shear while the metal-metal bonds are weakened and thus more easily accommodate shear. A clue for assessing the competing roles of these two types of bonds on shear resistance can be found in the amorphous structure, in which strongly bound metalloid-centered clusters are primarily joined to each other by relatively weak metal-metal bonds. As the metalloid content grows, the number of clusters increases, and clusters connect by sharing vertices, edges or faces. Such a picture of solute-centered clusters and sharing arrangements for metalloid-transition metal glass was shown by Sheng *et al.*[17] Molecular dynamics (MD) simulations[18] show a nearly complete absence of metalloid-metalloid neighbors over the range of metalloid content studied, and also show that increasing the metalloid content mainly increases the number of vertex-sharing clusters. Edge-sharing clusters increase to a lesser extent and face-sharing clusters remain few in number. In crystal structures, the latter type of clusters linkage enters at 33 at. % metalloid. Deformation studies[19] show that shear is easily accommodated when clusters are linked by metal-metal bonds. Among clusters in contact, shear is more readily accommodated by vertex- and edge-sharing clusters than by face-sharing clusters.

TABLE I. Thermal stability and mechanical properties of Fe–Cr–Mo–P–C–B BMGs. Symbols: σ_y=yield stress, σ_f=fracture strength, and ε_{pl}=plastic strain. G, K, E, and ν are defined in the text.

| Alloy	T_g (K)	T_x (K)	σ_y (GPa)	σ_f (GPa)	ε_{pl} (%)	G (GPa)	K (GPa)	E (GPa)	ν
$Fe_{68}Cr_3Mo_{10}P_6C_{10}B_3$	714	764	3.1	3.5	0.4	67.7	172	180	0.326
$Fe_{66}Cr_3Mo_{10}P_8C_{10}B_3$	721	769	3.1	3.4	1.1	66.5	172	177	0.330
$Fe_{64}Cr_3Mo_{10}P_{10}C_{10}B_3$	729	775	2.8	3.4	1.2	66.0	174	176	0.332
$Fe_{63}Cr_3Mo_{10}P_{12}C_{10}B_2$	735	778	2.6	3.4	3.2	65.3	178	178	0.336
$Fe_{63}Cr_3Mo_{10}P_{12}C_9B_3$	739	783	3.0	3.5	1.1	65.5	175	175	0.333
$Fe_{63}Cr_3Mo_{10}P_{12}C_8B_4$	745	793	3.0	3.4	1.2	65.5	174	175	0.333
$Fe_{63}Cr_3Mo_{10}P_{12}C_7B_5$	751	817	3.1	3.4	1.3	65.2	174	173	0.333
$Fe_{62}Cr_3Mo_{10}P_{12}C_{10}B_3$	744	793	3.0	3.4	2.9	64.6	172	172	0.332
$Fe_{60}Cr_3Mo_{10}P_{14}C_{10}B_3$	775	836	⋯	⋯	⋯	64.0	174	171	0.336
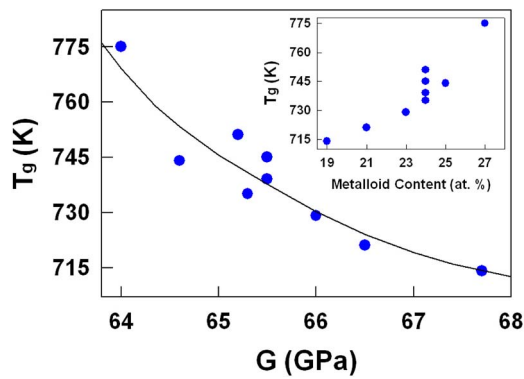
FIG. 3. (Color online) T_g vs G for Fe-BMGs listed in Table I. The curve is drawn as a guide for the eye. T_g vs total metalloid content is plotted in the inset.

FIG. 5. (Color online) ICOHP as a function of bond length for Fe–Fe and Fe–P bonds in Fe_3P (*tI*32 structure) compared with elemental Fe (*cI*2 structure). Lines are drawn as guides to the eye.

The observed composition dependence of G can be qualitatively interpreted as a tradeoff between opposing tendencies: a continual reduction in the strength of metal-metal bonds that persists over the composition range studied; a density of increasingly shear-resistant links between clusters that more rapidly grows as the metalloid content is near ~30 at.%. Therefore, G is expected to initially decrease with increasing metalloid content, reach a minimum, and then increase at higher metalloid fraction as the density of strong cluster contacts grows. Experimentally observed shear modulus trend and MD simulations both suggest that the present alloys remain below the threshold at which strong face-sharing linkages proliferate. The increase in number of more strongly linked clusters at increasing metalloid content increases the overall activation barrier for configuration changes of the glass to occur, resulting in an increase in T_g.

In summary, the mechanical properties and glass transition temperature of Fe–Cr–Mo–P–C–B BMGs that contain high metalloid content were studied. The alloys exhibit high plastic strain and fracture strength. The interdependences be-
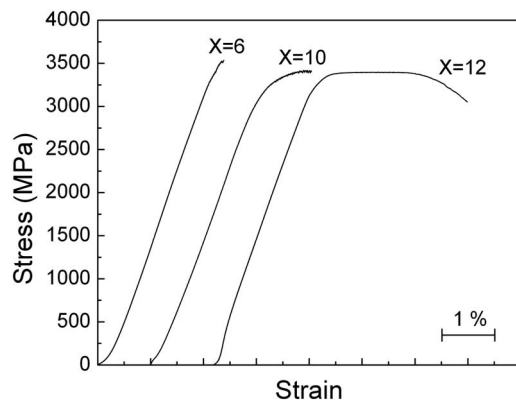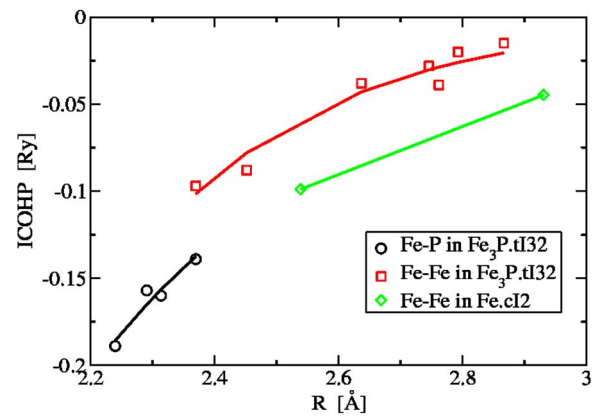
tween shear modulus, glass transition temperature, and metalloid content were found to exhibit unexpected trends. By employing first-principles electronic structure calculations, the results were attributed to the interplay of atomic bonding and cluster linkages in the amorphous network.

FIG. 4. Compressive true stress-strain curves for three $Fe_{74-x}Cr_3Mo_{10}C_{10}B_3P_x$ (x=6, 10, and 12) alloys.

[1] J. C. Dyre, Rev. Mod. Phys. **78**, 953 (2006).
[2] W. L. Johnson, M. D. Demetriou, J. S. Harmon, M. L. Lind, and K. Samwer, Mater. Res. Bull. **32**, 644 (2007).
[3] H. S. Chen, J. T. Krause, and E. Coleman, J. Non-Cryst. Solids **18**, 157 (1975).
[4] J. J. Lewandowski, W. H. Wang, and A. L. Greer, Philos. Mag. Lett. **85**, 77 (2005).
[5] J. Schroers and W. L. Johnson. Phys. Rev. Lett. **93**, 255506 (2004).
[6] X. J. Gu, A. G. McDermott, S. J. Poon, and G. J. Shiflet, Appl. Phys. Lett. **88**, 211905 (2006).
[7] X. J. Gu, S. J. Poon, and G. J. Shiflet, J. Mater. Res. **22**, 344 (2007).
[8] A. Castellero, D. I. Uhlenhaut, B. Moser, and J. F. Loffler, Philos. Mag. Lett. **87**, 383 (2007).
[9] W. H. Wang, J. Non-Cryst. Solids **351**, 1481 (2005).
[10] W. H. Wang, J. Appl. Phys. **99**, 093506 (2006).
[11] T. Egami, S. J. Poon, Z. Zhang, and V. Keppens, Phys. Rev. B **76**, 024203 (2007).
[12] G. Duan, M. L. Lind, K. D. Blauwe, A. Wiest, and W. L. Johnson, Appl. Phys. Lett. **90**, 211901 (2007).
[13] X. J. Gu, S. J. Poon, G. J. Shiflet, and M. Widom, Acta Mater. **56**, 88 (2008).
[14] G. Kresse and J. Furthmuller, Phys. Rev. B **54**, 11169 (1996).
[15] O. K. Andersen and O. Jepsen, Z. Phys. B: Condens. Matter **97**, 35 (1995).
[16] R. Dronskowski and P. E. Blochl, J. Phys. Chem. **97**, 8617 (1993).
[17] H. W. Sheng, W. K. Luo, F. M. Alamgir, J. M. Bai, and E. Ma, Nature (London) **439**, 419 (2006).
[18] P. Ganesh and M. Widom, Phys. Rev. B **77**, 014205 (2008); M. Widom, P. Ganesh, S. Kazimirov, D. Louca, and M. Mihalkovic, J. Phys.: Condens. Matter **20**, 114114 (2008).
[19] C. Jiang, S. G. Srinivasan, A. Caro, and S. A. Maloy, J. Appl. Phys. **103**, 043502 (2008).